

Research Article

Effect of Silver Nanoparticle Size on Efficiency Enhancement of Dye-Sensitized Solar Cells

Chanu Photiphitak,¹ Pattana Rakkwamsuk,¹ Pennapa Muthitamongkol,²
Chaiyuth Sae-Kung,³ and Chanchana Thanachayanont²

¹ School of Energy, Environment and Materials, Division of Materials Technology, King Mongkut's University of Technology Thonburi, 126, Pracha-utid Road, Bangmod, Toongkru, Bangkok 10150, Thailand

² National Metal and Material Technology Center, 114 Thailand Science Park, Phaholyothin Road, Klong 1, Klong Luang, Pathumthani 12120, Thailand

³ Institute of Solar Energy Technology Development, Phaholyothin Road, Pathumthani 12120, Thailand

Correspondence should be addressed to Chanchana Thanachayanont, chanchm@mtec.or.th

Received 13 December 2010; Revised 12 April 2011; Accepted 25 April 2011

Academic Editor: Vincenzo Augugliaro

Copyright © 2011 Chanu Photiphitak et al. This is an open access article distributed under the Creative Commons Attribution License, which permits unrestricted use, distribution, and reproduction in any medium, provided the original work is properly cited.

Titanium dioxide/silver (TiO₂/Ag) composite films were prepared by incorporating Ag in pores of mesoporous TiO₂ films using a photoreduction method. The Ag nanoparticle sizes were in a range of 4.36–38.56 nm. The TiO₂/Ag composite films were characterized by X-ray diffraction (XRD), scanning electron microscopy (SEM) and transmission electron microscopy (TEM). The TiO₂ and TiO₂/Ag composite films were then sensitized by immersing in a 0.3 mM N719 dye solution and fabricated for conventional dye-sensitized solar cells (DSCs). *J-V* characteristics of the TiO₂/Ag DSCs showed that the Ag nanoparticle size of 19.16 nm resulted in the short circuit current density and efficiency of 8.12 mA/cm² and 4.76%.

1. Introduction

Surface plasmon resonance induced by silver (Ag) nanoparticles leads to an increase in an absorption coefficient of dye in dye-sensitized solar cells (DSCs) [1–6]. The effect has been theoretically described as an increase of local electromagnetic field nearby metal surfaces which is found when wavelengths of irradiation sources are correlated with the optical absorption of the surface plasmon resonance [7–11]. The modification of the surfaces for an enhancement of optical absorption, hence, provides a good method to improve efficiency of an optoelectronic device involving photon absorption [12]. Several methods for the fabrication of the silver nanoparticles were studied such as thermal evaporation of Ag islands on titanium dioxide (TiO₂) films [1], magnetron sputtering of TiO₂ and Ag composite films [13], electrochemical deposition of Ag by double pulse method on indium tin oxide (ITO) [14], loading of Ag and silver chloride (AgCl) onto anatase TiO₂ nanotubes that were

grown by a hydrothermal treatment [15] and loading of the Ag nanoparticles onto self-organized TiO₂ nanotube layers using photocatalytic reduction [16, 17].

Wen et al. [1] generated the Ag island films by depositing the 3.3–6.0 nm-thick Ag nanoparticle layer on the TiO₂ film electrode using thermal evaporation and found a possibility of using plasmon resonance effect to enhance the efficiency of the DSCs, if the volume and structure of the Ag island films could be controlled and optimized. Ihara et al. [18] improved photoelectric conversion efficiency of their dye-sensitized solar cells by using localized surface plasmon of the Ag nanoparticles (diameter of 12.5 nm) modified with polymer and reported that the efficiency of dye-sensitized solar cell with the Ag nanoparticles increased from 1.5% to 2.5% compared with the case with no Ag nanoparticles. Chen et al. [19] studied effects of adding silver nanowires (40 nm in diameter and 20 μm in length) in the anode of the DSCs to improve the photovoltaic efficiency. Results showed that the composite anode of Ag nanowires and TiO₂/P25 has

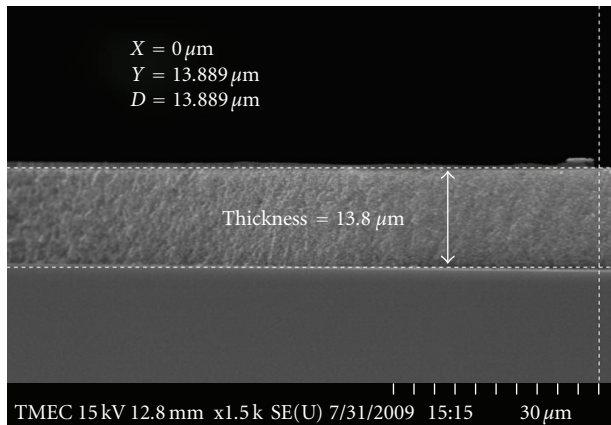


FIGURE 1: An SEM image showing a cross-section of the TiO_2 film.

improved photovoltaic conversion efficiency about two times of standard P-25 DSCs. Chou et al. [20] prepared TiO_2/Ag composite particles by dry particle-coating technique. The Ag particle size was bigger than 100 nm, and the TiO_2/Ag composite particles were found to improve the efficiency of the DSCs because Schottky barrier exceeded that of the conventional DSCs.

In this study, for a cost-effective process, we prepared the Ag nanoparticles with sizes in a range of 4.36–38.56 nm using a photoreduction method. The Ag nanoparticles were deposited onto the mesoporous anatase TiO_2 electrode with worm-like pores. The Ag nanoparticles were incorporated thoroughly into the pores of the mesoporous TiO_2 film electrode [21–24]. The effect of the Ag nanoparticle size on the efficiency enhancement of dye-sensitized solar cells was investigated. The optimum DSC in this study showed a maximum efficiency of 4.76%. Although the 5.45% efficiency by using a similar material ($\text{TiO}_2/\text{Ag}/\text{DSC}$) has been showed in 2007 by Ramasamy et al. [25], this is the first time that the effect of Ag particle sizes is carefully investigated.

2. Materials and Methods

2.1. The Preparation of Mesoporous TiO_2 Electrodes. The TiO_2 electrodes were screen printed from a TiO_2 paste (Dyesol) 3 times on a fluorine-doped tin oxide (FTO) glass substrate ($2 \times 3 \text{ cm}^2$ in size). A 200 mesh was used to obtain a TiO_2 layer with area of $0.5 \times 1.2 \text{ cm}^2$ and a thickness of approximately $13.8 \mu\text{m}$ (see Figure 1). In order to avoid contamination on the fresh film, screen printing was performed in a clean-room environment. After drying at 55°C for 30 minutes, the electrodes were sintered at 450°C for 30 minutes, and then cooled down to room temperature. The electrodes were immersed in a $3 \times 10^{-4} \text{ M}$ of N719 dye solution, namely, cis-diisothiocyanato-bis(2,2-bipyridyl-4,4-dicarboxylatoe) ruthenium (II)bis (tetrabutylammonium) in absolute ethanol for 24 hours. The excess dye was removed from the electrode by rinsing with ethanol.

2.2. The Synthesis of Mesoporous TiO_2/Ag Films. In order to deposit the Ag nanoparticles on the TiO_2 film, a $2 \times 3 \text{ cm}^2$

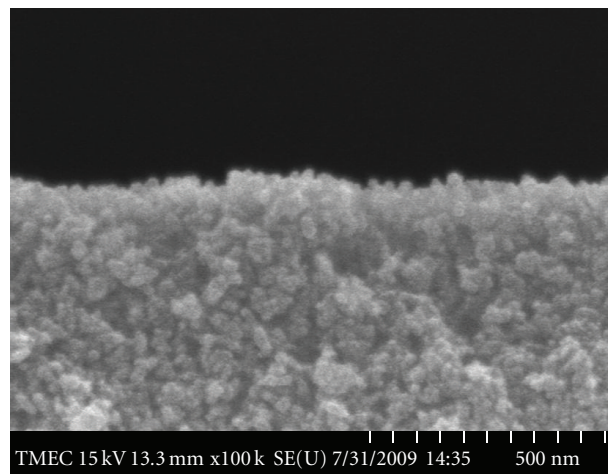
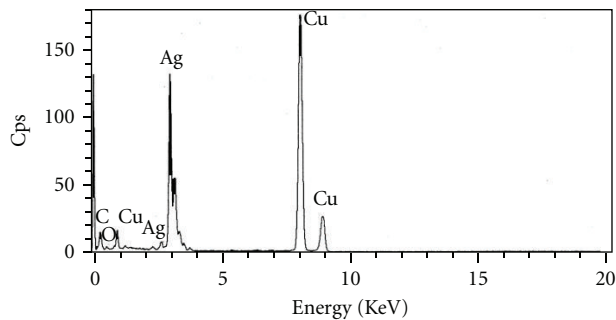


FIGURE 2: An SEM cross-sectional micrograph of the TiO_2/Ag composite film with a UV exposure for 120 minutes. Inset shows an EDX spectrum indicating the presence of the Ag nanoparticles on the TiO_2 films.

FTO glass with $0.5 \times 1.2 \text{ cm}^2$ TiO_2 films was immersed in the 0.1 M AgNO_3 solution for five seconds, then rinsed with DI water and dried in a N_2 stream. The films were then exposed to a UV irradiation at $\lambda = 254 \text{ nm}$ using a Spectroline CM-10 Fluorescence Analysis Cabinet at an intensity of $\sim 0.31 \text{ mW}/\text{cm}^2$. We designed the experiment to vary exposure times for 5, 10, 15, 20, 30, 60, 90, 120, 150, 180, and 240 minutes for the photocatalytic reduction of Ag^+ to the metallic Ag nanoparticles. Finally, the TiO_2/Ag electrodes were immersed in dye solution for 24 hours and prepared for dye-sensitized solar cells.

2.3. The Preparation of Pt Counter Electrodes. The counter electrodes were prepared by screen printing a thin layer of platinum (Pt) with a size of $0.5 \times 1.2 \text{ cm}^2$ using a platinum paste (Dyesol), on an FTO glass substrate ($2 \times 3 \text{ cm}^2$), and then sintered at 450°C for 30 minutes.

2.4. DSC Fabrication. A sandwich-type cell [26] was fabricated by assembling a sensitized TiO_2 electrode using surlyn-based polymer sheet ($80 \mu\text{m}$ thick) and sealed by a hot gun for a few seconds. The liquid electrolyte contained 0.5 M LiI, 0.05 M I_2 , and 0.5 M 4-tert-butyl pyridine in 90:10 v/v of acetonitrile: 3 methyl-2-oxazolidinone. Electrolyte-injecting holes, made on the counter-electrode side, were sealed with surlyn and glass cover.

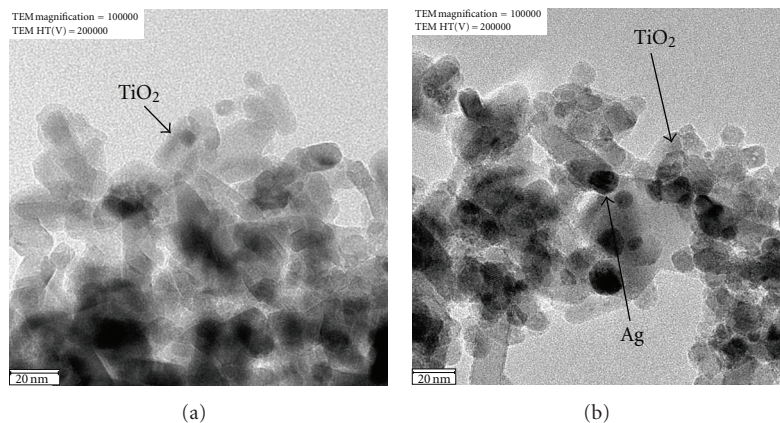


FIGURE 3: TEM micrographs of the TiO_2 nanotubes (a) before and (b) after immersion in the AgNO_3 solution with UV exposure for 120 minutes.

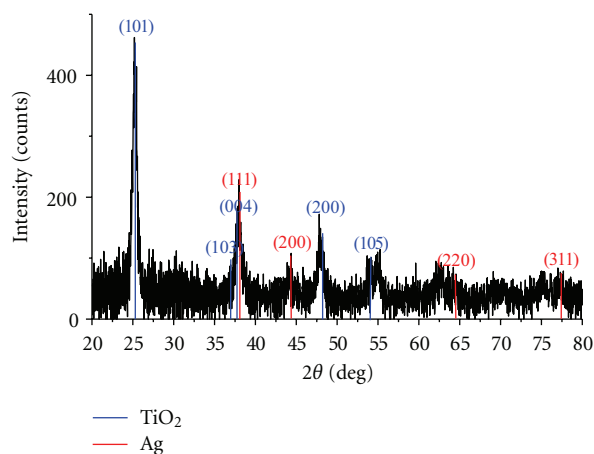


FIGURE 4: XRD peaks of the TiO_2/Ag composite film with UV exposure for 120 minutes on an FTO glass substrate. (Note: graph plotted by OriginLab software program.)

2.5. Measurements. Optical absorption spectra of the film electrode samples were measured using a UV-visible spectrophotometer (Jasco model: V-530). In order to observe the microstructure and elemental analysis of the obtained Ag nanoparticles, the Ag nanoparticles were prepared on carbon-coated copper grids for observations by transmission electron microscopy (TEM JEOL model JSM-2010). The X-ray diffraction (XRD JEOL-300) patterns were obtained by analyzing the Ag/TiO_2 films on the glass substrates. Scanning electron microscope (SEM JEOL model: JSM-6301 F) was employed to record cross-sectional micrographs of the Ag/TiO_2 films. J - V measurements were performed under a 450 W xenon light source which is able to provide $1000 \text{ W} \cdot \text{m}^{-2}$ sunlight equivalent irradiation (AM 1.5), using Keithley digital source meter (Model 2400) under the illuminated condition.

3. Results and Discussion

3.1. Morphology of the TiO_2/Ag Deposited Films. The TiO_2 films were prepared by screen printing 3 layers of the TiO_2

paste and calcination at 450°C for 30 minutes. A thickness measured using SEM is approximately $13.8 \mu\text{m}$ as shown in Figure 1 (in agreement with [27–30]).

The TiO_2 films were loaded with the Ag nanoparticles using the AgNO_3 soaking and the UV illumination treatment described in the experimental part 2.2. After the films were irradiated by the UV light, they turned brownish grey in a few minutes due to photocatalytic reduction of Ag^+ to Ag [31]. The Ag nanoparticles on the TiO_2 particles were not readily observed by the SEM (Figure 2). However, The TiO_2/Ag composite films were characterized using energy dispersive X-Ray spectroscopy (EDX) technique attached to the SEM. We found that the peaks of the Ag nanoparticles were present (Figure 2), suggesting the presence of the Ag nanoparticles on surface of the TiO_2 films.

Figure 3(a) shows a TEM micrograph of the TiO_2 nanoparticles from the TiO_2 films before immersion in the AgNO_3 solution. We found that the TiO_2 nanoparticles were nanorods and the lengths were approximately 25 nm. Figure 3(b) shows an example of the TEM images of the TiO_2 nanorods from the films after immersion in the AgNO_3 solution and exposed to the UV irradiation for 120 minutes. The result shows the presence of the TiO_2 nanorods and the spherical Ag nanoparticles adsorbed on surfaces of the TiO_2 nanorods. An example of XRD pattern of the TiO_2/Ag composite films (Figure 4) shows that four 2θ diffraction peaks at 38.12, 44.30, 64.44, and 77.40 could, respectively, be indexed as (111), (200), (220), and (311) planes of face-centered cubic Ag. Peaks at 25.36, 37.05, 37.90, 48.15, and 54.05 are indexed as (101), (103), (004), (200), and (105) planes of the anatase TiO_2 .

The Ag nanoparticles were also prepared on the carbon-coated copper grids and exposed to varied UV exposure times of 0, 5, 10, 15, 20, 30, 60, 90, 120, 150, 180 and 240 minutes. The average diameters of the Ag nanoparticles measured from the TEM micrographs using Image-Pro Plus 5.0 software program were approximately 4.36 ± 2.53 , 4.56 ± 1.78 , 5.39 ± 1.83 , 6.20 ± 1.65 , 7.17 ± 2.59 , 10.98 ± 1.80 , 15.57 ± 3.26 , 19.16 ± 3.71 , 23.55 ± 4.26 , 27.51 ± 8.05 , and 38.56 ± 5.30 , respectively. The sizes of Ag nanoparticles were found to depend strongly on the UV exposure time (Figure 5) due to

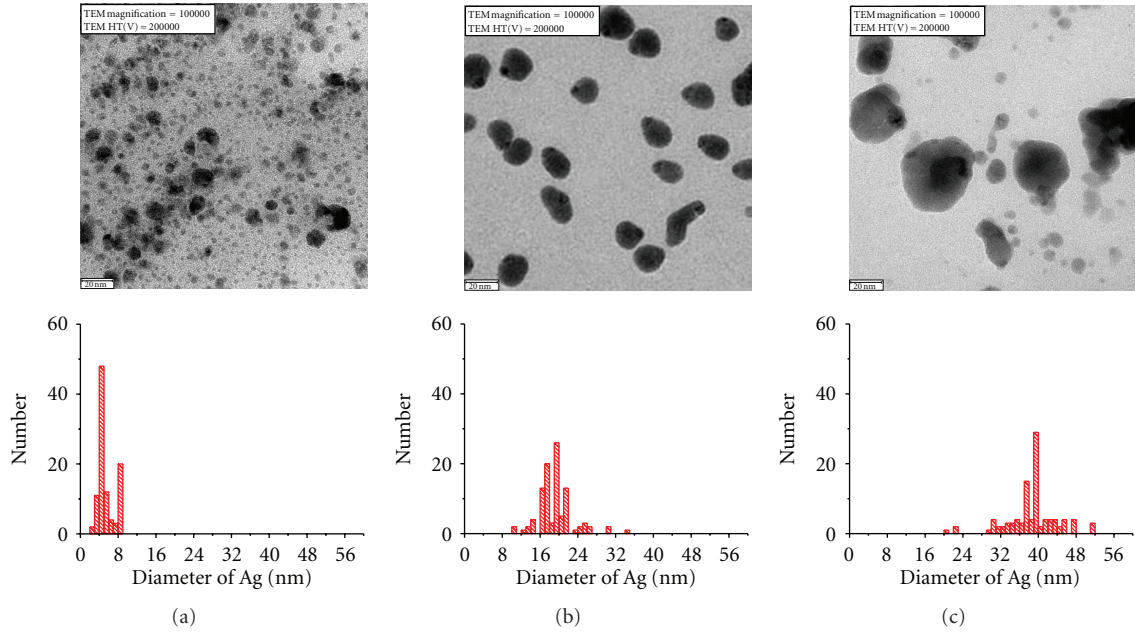


FIGURE 5: TEM micrographs and size distributions of silver nanoparticles prepared by photocatalytic reduction in a 0.1 M AgNO_3 solution on the carbon-coated copper grids at UV exposure times of (a) 5 minutes, (b) 120 minutes, and (c) 240 minutes, respectively. The average size increases and the distribution broadens with an increase in the UV exposure time. (Note: graph plotted by OriginLab software program).

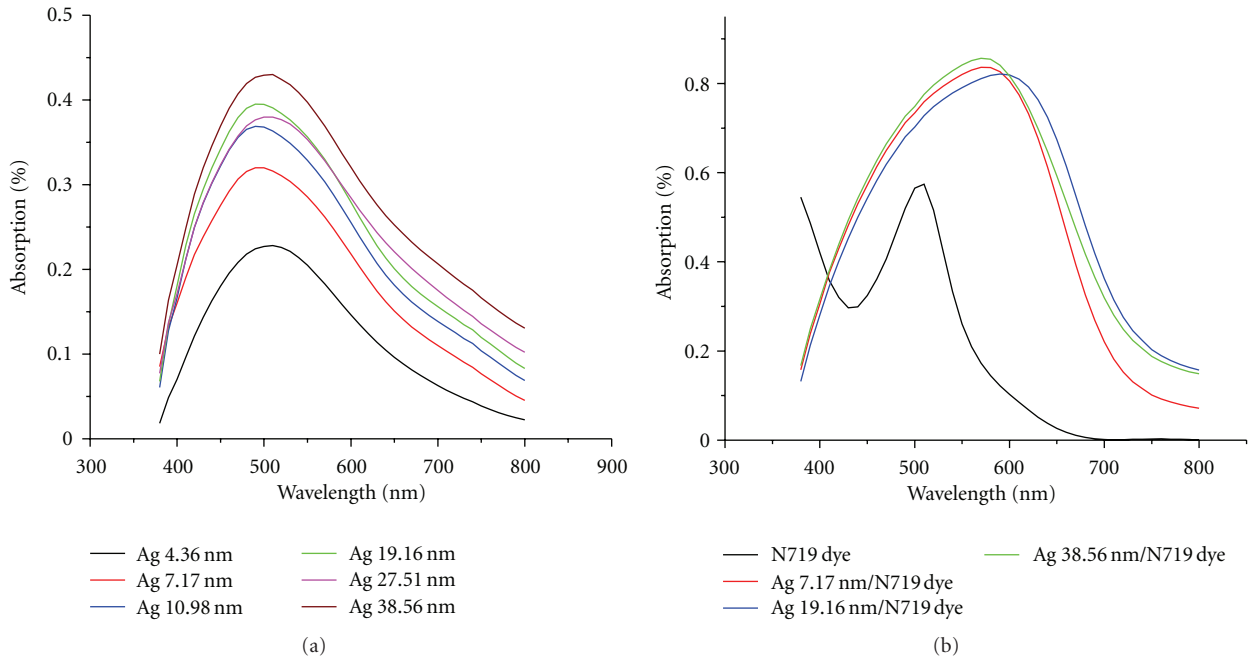


FIGURE 6: Optical absorption spectra of: (a) the Ag nanoparticle films with various particle sizes of the Ag nanoparticles in the range of 4.36–38.56 nm and (b) the Ag/N719 dye film compared with an optical absorption spectrum of 3×10^{-5} M N719 dye solution.

the photocatalytic reduction of the Ag^+ to the Ag metal in the form of the Ag nanoparticles where electrons were provided by water [17, 31].

3.2. The Effect of the Ag Nanoparticle Size on Optical Absorption Spectra. The absorption spectrum of the Ag nanoparticles exhibits the surface plasmon peak at approximately 400 nm on the broad band [32]. Optical absorption spectra

can be theoretically calculated using Mie's theory. When the particles having diameter (R) are suspended in a medium with the dielectric constant (ϵ_m), the dipolar absorption efficiency (Q_{abs}) is given by

$$Q_{\text{abs}} = \frac{24\pi R}{\lambda} \cdot \frac{\epsilon_m^{3/2} \epsilon''(\omega)}{\epsilon''(\omega)^2 + \langle \epsilon'(\omega) + 2\epsilon_m + 48\pi^2 R^2 \epsilon_m^2 / 5\lambda^2 \rangle^2}, \quad (1)$$

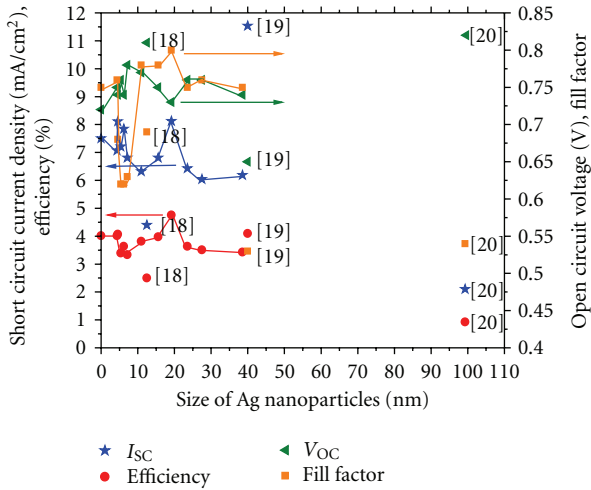


FIGURE 7: Open circuit voltages (V_{OC}), short circuit current densities (J_{SC}), fill factors (FF), and efficiencies of the DSCs with varied sizes of the Ag nanoparticles compared with reported DSCs [18–20]. At [18], use $2\ \mu\text{m}$ of TiO_2 thickness and size of $0.25\ \text{cm}^2$, [19] use $15\ \mu\text{m}$ of TiO_2 thickness and size of $0.25\ \text{cm}^2$, [20] use $8.1\ \mu\text{m}$ of TiO_2 thickness and size of $4.0\ \text{cm}^2$, and this study uses $13.8\ \mu\text{m}$ of TiO_2 thickness and size of $0.6\ \text{cm}^2$.

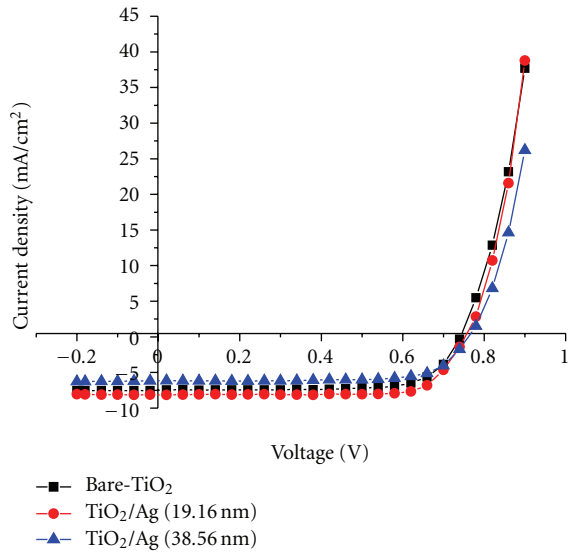


FIGURE 8: J - V characteristics of the DSCs composed of the TiO_2 electrodes with N719 dye before and after improvement with the Ag nanoparticles.

where λ is a wavelength of the incoming light in the medium, and $\varepsilon'(\omega)$ and $\varepsilon''(\omega)$ represent the real and imaginary parts of the dielectric function, $\varepsilon(\omega)$, respectively, [$\varepsilon(\omega) = \varepsilon'(\omega) + \varepsilon''(\omega)$]. Thus, the absorption efficiency of particles is a function of the dielectric constant of the metal, that of medium and the size of the particle.

From (1), the Mie's theory only successfully explains the absorption band for metallic nanoparticles in visible range, and, for radius less than 5 nm, the width of the surface plasmon peak increases linearly with the reciprocal of the

radius [32, 33]. On the other hand, the width of the surface plasmon peak increases with an increase in the radius in the range larger than 10 nm, because of inhomogeneous polarization of the particles in the electromagnetic field of the incoming light due to excitation of a different multiple modes which makes a peak in the spectrum at a different energy [32, 34]. Figure 6(a) shows optical absorption spectra of the Ag nanoparticles films indicating an increase in wavelength (red shifted) with an increase in the diameters of the Ag nanoparticles because the width of the surface plasmon peak increases.

Figure 6(b) shows the absorption peak of the Ag/N719 dye film, it is found that the Ag 19.16 nm/N719 dye film has a maximum peak width or red shift due to the surface plasmon resonance of the silver particles contributing to the absorption coefficient of the dye. The absorption of the Ru-dye can occur via the metal-ligand charge-transfer transition (MLCT), $t_2 \rightarrow \pi^*$ MLCT transitions in the absorption maximum at 396 and 534 nm, and $\pi \rightarrow \pi^*$ intraligand transition in the UV [35]. Thus, both the surface Plasmon resonance absorption of Ag nanoparticles and the Ru-dye absorption for MLCT transition contributed to the total absorption.

3.3. The Effect of the Ag Nanoparticle Size on Efficiency of the DSCs. Parameters extracted from J - V characteristics, for example, Figure 8, of the TiO_2/Ag composite film electrode DSCs are shown in Table 1. The Ag nanoparticles of the average size of 19.16 nm (3.59 ± 0.50 weight % of Ag nanoparticles in the TiO_2/Ag composite) were found to result in the maximum value of short circuit current density of $8.12\ \text{mA}/\text{cm}^2$.

As shown in Table 1, the pure TiO_2 electrode (reference cell) results in the short circuit current density (J_{SC}) of $7.50\ \text{mA}/\text{cm}^2$, open circuit voltages (V_{OC}) of 0.72 V, fill factors (FF) of 0.75, and efficiency of 4.02%. For the TiO_2/Ag electrodes, after improvement with intercalation of Ag nanoparticles of which size ranging from 4.36 to 38.56 nm, we found that the dye-sensitized solar cell which was prepared from the TiO_2/Ag (19.16 nm) electrode had maximum values of the J_{SC} , FF, and efficiency of $8.12\ \text{mA}/\text{cm}^2$, 0.80 and 4.76%, respectively, with V_{OC} of 0.73. Compared with the reference cell, the TiO_2/Ag (19.16 nm) is found to improve J_{SC} , FF, and efficiency because of an optimum electromagnetic field introduced by the silver plasmon resonance that enhances the optical absorption of the dye [2, 3, 36]. The other possible reason is that the Ag nanoparticles have a catalytic effect that increases the reaction rate between the semiconductor, dye, and the redox electrolyte and/or the internal photoemission from the Ag nanoparticles increases the photocurrent [1, 3, 36]. However, the dye-sensitized solar cells which were prepared from the TiO_2/Ag electrodes with the Ag nanoparticle sizes bigger than 19.16 nm have low values of the J_{SC} . It is believed that with the Ag particle sizes bigger than 19.16 nm, Schottky barriers formed at the TiO_2/Ag contacts become dominant and retard electron transport in the conduction bands [1, 3, 37, 38].

Figure 7 plots J_{SC} , V_{OC} , FF, and efficiencies versus the sizes of the Ag nanoparticles. The DSCs in our study were

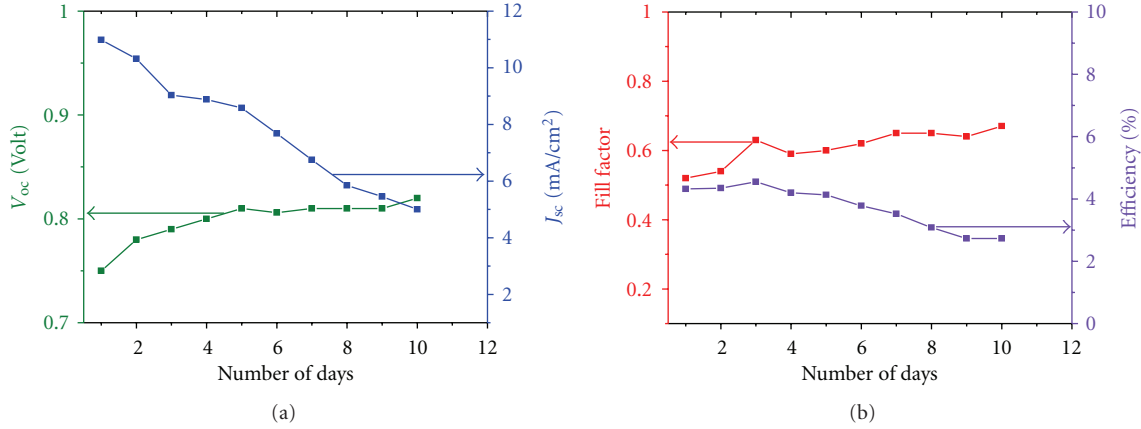


FIGURE 9: Variation of (a) open-circuit voltage (V_{OC}) and short-circuit current density (J_{SC}), (b) fill factor (FF) and energy conversion efficiency of DSC with TiO_2/Ag (19.16 nm) electrode during a short-term stability test.

TABLE 1: Weight (%) of Ag nanoparticles obtained from SEM-EDX analysis, short circuit current densities (J_{SC}), open circuit voltages (V_{OC}), fill factors (FF), and efficiencies of DSCs prepared using the TiO_2/Ag composite film electrodes compared with pure TiO_2 electrode (reference) under AM1.5.

No.	Size of Ag nanoparticles on TiO_2 electrode (nm)	Weight (%) of Ag nanoparticles	J_{SC} (mA/cm ²)	V_{OC} (V)	FF	Efficiency (%)
1	pure TiO_2 (reference)	0	7.50	0.72	0.75	4.02
2	4.36 ± 2.53	3.30 ± 0.35	7.07	0.75	0.76	4.02
3	4.56 ± 1.78	4.01 ± 0.56	8.11	0.74	0.68	4.07
4	5.39 ± 1.83	3.52 ± 0.27	7.21	0.76	0.62	3.40
5	6.20 ± 1.65	3.45 ± 0.30	7.84	0.74	0.62	3.64
6	7.17 ± 2.59	3.56 ± 0.30	6.81	0.78	0.63	3.34
7	10.98 ± 1.80	3.54 ± 0.38	6.32	0.77	0.78	3.82
8	12.5 [18]	—	4.40	0.81	0.69	2.5
9	15.57 ± 3.26	3.29 ± 0.11	6.81	0.75	0.78	3.98
10	19.16 ± 3.71	3.59 ± 0.50	8.12	0.73	0.80	4.76
11	23.55 ± 4.26	4.14 ± 0.94	6.43	0.76	0.75	3.64
12	27.51 ± 8.05	4.20 ± 0.34	6.04	0.76	0.76	3.51
13	38.56 ± 5.30	4.42 ± 0.45	6.19	0.74	0.75	3.43
14	40 [19]	—	11.53	0.65	0.53	4.10
15	~100 [20]	—	2.10	0.82	0.54	0.93

compared with the Ag nanoparticle size of around 12.5 [18], 40 [19], and 100 [20] nm on the TiO_2 electrodes reported elsewhere. Due to different thicknesses of the TiO_2 layers prepared, direct comparison cannot be made. However, the improved J_{SC} of the best DSC prepared in this study is noteworthy. Compared with the reported DSCs with the Ag nanowires of 40 nm in diameter and 20 μm in length [19] with the J_{SC} of 11.53 mA/cm², the best DSC in this study has a lower value of J_{SC} . The high value of J_{SC} in the Ag nanowire DSCs has been reported to be due to metal network formation by adding Ag nanowires to improve the production and transportation of photon-generated current [39].

However the V_{OC} , FF, and efficiency values of the Ag nanowire DSCs are not higher than the best value reported

in this study. When compared with the reported DSCs with the Ag nanoparticle size of around 100 nm [20], the values of J_{SC} , V_{OC} , FF and Efficiency follow a decreasing trend after the maximum values because the Schottky barriers formed at the TiO_2/Ag contact retarding electron transport in conduction bands [1, 3]. Therefore, the Ag nanoparticles size of 19.16 nm prepared in this study is an appropriate size to improve J_{SC} of the DSCs.

Figure 8 shows the J - V characteristics of the DSCs before and after improvement by the intercalation of the Ag nanoparticles into the TiO_2 electrodes. The optimum size of the Ag nanoparticle of 19.16 nm was found to give the maximum J_{SC} and the maximum efficiency of the DSCs. The intercalation of the Ag nanoparticles to the TiO_2 layer has been shown not to significantly affect values of V_{OC} , Figure 7,

because the V_{OC} is determined by the redox potential and the Fermi energy of semiconductors [1, 36], which do not change significantly with the change in size of the Ag nanoparticles.

Figure 9 shows the short-term stability of the dye-sensitized solar cells which were kept in an ambient atmosphere. The J - V characteristics of dye-sensitized solar cell using the Ag nanoparticle size of 19.16 nm on the TiO_2 electrode were measured at 24 h interval. It was found that the efficiency of the dye-sensitized solar cells was slightly enhanced in the first 3 days because of the increases in V_{OC} and FF increase. However, from the 4th day, the efficiency of dyesensitized of solar cells began to decrease because of the decrease in short circuit current density. This could be due to the instability of the Ag nanoparticles in the I^-/I_3^- redox electrolyte [1].

4. Conclusion

The DSCs composed of mesoporous TiO_2 films, N719 Ru dye and the redox of I^-/I_3^- were prepared and improved by the intercalation of the Ag nanoparticles into the TiO_2 electrodes by photoreduction method. The Ag nanoparticles were face centered cubic and varied in size in the range of 4.36–38.65 nm. The TiO_2 /Ag composite films were characterized by XRD, SEM, TEM and UV-Vis Spectrophotometer. The optimum size of the Ag nanoparticles was 19.16 nm giving the maximum J_{SC} and efficiency of 8.12 mA/cm² and 4.76%, respectively.

Acknowledgments

The authors thank the National Metal and Materials Technology Center (MTEC) and Institute of Solar Energy Technology Development (SOLARTEC), Thailand for financial support.

References

- [1] C. Wen, K. Ishikawa, M. Kishima, and K. Yamada, "Effects of silver particles on the photovoltaic properties of dye-sensitized TiO_2 thin films," *Solar Energy Materials and Solar Cells*, vol. 61, no. 4, pp. 339–351, 2000.
- [2] K. C. Lee, S. U. J. Lin, C. H. Lin, C. S. Tsai, and Y. J. Lu, "Size effect of Ag nanoparticles on surface plasmon resonance," *Surface and Coatings Technology*, vol. 202, no. 22–23, pp. 5339–5342, 2008.
- [3] G. Zhao, H. Kozuka, and T. Yoko, "Effects of the incorporation of silver and gold nanoparticles on the photoanodic properties of rose bengal sensitized TiO_2 film electrodes prepared by sol-gel method," *Solar Energy Materials and Solar Cells*, vol. 46, no. 3, pp. 219–231, 1997.
- [4] A. M. Glass, P. F. Lioa, J. G. Bergman, and D. H. Olson, "Interaction of metal particles with adsorbed dye molecules: absorption and luminescence," *Optics Letters*, vol. 5, pp. 368–3707, 1980.
- [5] Z. Y. Zhu, C. Mao, R. Y. Yang, L. X. Dai, and C. S. Nie, "Surface-enhanced Raman scattering of Ru(II) homo- and heterolytic complexes with 2,2'-bipyridine and 1,1'-biisoquinoline in aqueous silver sol," *Journal of Raman Spectroscopy*, vol. 24, pp. 221–226, 1993.
- [6] W. J. Yoon, K. Y. Jung, J. Liu et al., "Plasmon-enhanced optical absorption and photocurrent in organic bulk heterojunction photovoltaic devices using self-assembled layer of silver nanoparticles," *Solar Energy Materials and Solar Cells*, vol. 94, no. 2, pp. 128–132, 2010.
- [7] D. M. Schaadt, B. Feng, and E. T. Yu, "Enhanced semiconductor optical absorption via surface plasmon excitation in metal nanoparticles," *Applied Physics Letters*, vol. 86, no. 6, Article ID 063106, pp. 1–3, 2005.
- [8] C. F. Eagen, "Nature of the enhanced optical absorption of dye-coated Ag island films," *Applied Optics*, vol. 20, no. 17, pp. 3035–3042, 1981.
- [9] J. J. Mock, M. Barbic, D. R. Smith, D. A. Schultz, and S. Schultz, "Shape effects in plasmon resonance of individual colloidal silver nanoparticles," *Journal of Chemical Physics*, vol. 116, no. 15, pp. 6755–6759, 2002.
- [10] P. Royer, J. P. Goudonnet, R. J. Warmack, and T. L. Ferrell, "Substrate effects on surface-plasmon spectra in metal-island films," *Physical Review B*, vol. 35, no. 8, pp. 3753–3759, 1987.
- [11] G. Xu, M. Tazawa, P. Jin, S. Nakao, and K. Yoshimura, "Wavelength tuning of surface plasmon resonance using dielectric layers on silver island films," *Applied Physics Letters*, vol. 82, no. 22, pp. 3811–3813, 2003.
- [12] M. Ihara, K. Tanaka, K. Sakaki, I. Honma, and K. Yamada, "Enhancement of the absorption coefficient of cis-(NCS)₂ bis(2,2'-bipyridyl-4,4'-dicarboxylate)ruthenium(II) dye in dye-sensitized solar cells by a silver island film," *Journal of Physical Chemistry B*, vol. 101, no. 26, pp. 5153–5157, 1997.
- [13] J. Okumu, C. Dahmen, A. N. Sprafke, M. Luysberg, G. von Plessen, and M. Wuttig, "Photochromic silver nanoparticles fabricated by sputter deposition," *Journal of Applied Physics*, vol. 97, no. 9, Article ID 094305, pp. 1–6, 2005.
- [14] G. Sandmann, H. Dietz, and W. Plieth, "Preparation of silver nanoparticles on ITO surfaces by a double-pulse method," *Journal of Electroanalytical Chemistry*, vol. 491, no. 1–2, pp. 78–86, 2000.
- [15] L. Miao, Y. Ina, S. Tanemura et al., "Fabrication and photochromic study of titanate nanotubes loaded with silver nanoparticles," *Surface Science*, vol. 601, no. 13, pp. 2792–2799, 2007.
- [16] C. He, Y. A. Xiong, J. Chen, C. Zha, and X. Zhu, "Photoelectrochemical performance of Ag- TiO_2 /ITO film and photoelectrocatalytic activity towards the oxidation of organic pollutants," *Journal of Photochemistry and Photobiology A: Chemistry*, vol. 157, no. 1, pp. 71–79, 2003.
- [17] H. Hidaka, H. Honjo, S. Horikoshi, and N. Serpone, "Photoinduced Ag_n^0 cluster deposition. Photoreduction of Ag^+ ions on a TiO_2 -coated quartz crystal microbalance monitored in real time," *Sensors and Actuators, B*, vol. 123, no. 2, pp. 822–828, 2007.
- [18] M. Ihara, M. Kanno, and S. Inoue, "Photoabsorption-enhanced dye-sensitized solar cell by using localized surface plasmon of silver nanoparticles modified with polymer," *Physica E*, vol. 42, pp. 2867–2871, 2010.
- [19] T. Y. Chen, C. M. Fan, J. Y. Wu, and T. L. Lin, "Hybrid silver nanowire/titanium oxides nanocomposites as anode for dye-sensitized solar cell application," *Journal of the Chinese Chemical Society*, vol. 56, no. 6, pp. 1244–1249, 2009.
- [20] C. S. Chou, R. U. Y. Yang, C. K. Yeh, and Y. J. Lin, "Preparation of TiO_2 /Nano-metal composite particles and their applications in dye-sensitized solar cells," *Powder Technology*, vol. 194, no. 1–2, pp. 95–105, 2009.
- [21] I. Paramasivam, J. M. Macak, A. Ghicov, and P. Schmuki, "Enhanced photochromism of Ag loaded self-organized TiO_2

- nanotube layers,” *Chemical Physics Letters*, vol. 445, no. 4-6, pp. 233–237, 2007.
- [22] Y. Liu, X. Wang, F. Yang, and X. Yang, “Excellent antimicrobial properties of mesoporous anatase TiO₂ and Ag/TiO₂ composite films,” *Microporous and Mesoporous Materials*, vol. 114, no. 1-3, pp. 431–439, 2008.
- [23] S. K. Lim, S. K. Lee, S. H. Hwang, and H. Kim, “Photocatalytic deposition of silver nanoparticles onto organic/inorganic composite nanofibers,” *Macromolecular Materials and Engineering*, vol. 291, no. 10, pp. 1265–1270, 2006.
- [24] K. Naoi, Y. Ohko, and T. Tatsuma, “TiO₂ films loaded with silver nanoparticles: control of multicolor photochromic behavior,” *Journal of the American Chemical Society*, vol. 126, no. 11, pp. 3664–3668, 2004.
- [25] E. Ramasamy, W. J. Lee, D. Y. Lee, and J. S. Song, “Portable, parallel grid dye-sensitized solar cell module prepared by screen printing,” *Journal of Power Sources*, vol. 165, no. 1, pp. 446–449, 2007.
- [26] M. K. I. Senevirathna, P. K. D. D. P. Pitigala, E. V. A. Premalal, K. Tennakone, G. R. A. Kumara, and A. Konno, “Stability of the SnO₂/MgO dye-sensitized photoelectrochemical solar cell,” *Solar Energy Materials and Solar Cells*, vol. 91, no. 6, pp. 544–547, 2007.
- [27] S. K. Deb, “Dye-sensitized TiO₂ thin-film solar cell research at the national renewable energy laboratory (NREL),” *Solar Energy Materials and Solar Cells*, vol. 88, no. 1, pp. 1–10, 2005.
- [28] J. Jiu, S. Isoda, M. Adachi, and F. Wang, “Preparation of TiO₂ nanocrystalline with 3-5 nm and application for dye-sensitized solar cell,” *Journal of Photochemistry and Photobiology A*, vol. 189, no. 2-3, pp. 314–321, 2007.
- [29] K. Onoda, S. Ngamsinlapasathian, T. Fujieda, and S. Yoshikawa, “The superiority of Ti plate as the substrate of dye-sensitized solar cells,” *Solar Energy Materials and Solar Cells*, vol. 91, no. 13, pp. 1176–1181, 2007.
- [30] J. Kallioinen, M. R. Hassan, G. S. Paraoanu, and J. Korppi-Tommola, “Dye-sensitized nanostructured TiO₂ film based photoconductor,” *Journal of Photochemistry and Photobiology A*, vol. 195, no. 2-3, pp. 352–356, 2008.
- [31] Y. Ohko, T. Tatsuma, T. Fujii et al., “Multicolour photochromism of TiO₂ films loaded with silver nanoparticles,” *Nature Materials*, vol. 2, no. 1, pp. 29–31, 2003.
- [32] F. Mafuné, J. Y. Kohno, Y. Takeda, T. Kondow, and H. Sawabe, “Formation and size control of silver nanoparticles by laser ablation in aqueous solution,” *Journal of Physical Chemistry B*, vol. 104, no. 39, pp. 9111–9117, 2000.
- [33] D. K. Bhui, H. Bar, P. Sarkar, G. P. Sahoo, S. P. De, and A. Misra, “Synthesis and UV-vis spectroscopic study of silver nanoparticles in aqueous SDS solution,” *Journal of Molecular Liquids*, vol. 145, no. 1, pp. 33–37, 2009.
- [34] R. Das, S. S. Nath, D. Chakdar, G. Gope, and R. Bhattacharjee, “Preparation of silver nanoparticles and their characterization,” *Journal of Nanotechnology*, vol. 5, pp. 1–6, 2009.
- [35] D. S. Wang and M. Kerker, “Enhanced Raman scattering by molecules adsorbed at the surface of colloidal spheroids,” *Physical Review B*, vol. 24, no. 4, pp. 1777–1790, 1981.
- [36] K. Ishikawa, C. J. Wen, K. Yamada, and T. Okubo, “The photocurrent of dye-sensitized solar cells enhanced by the surface plasmon resonance,” *Journal of Chemical Engineering of Japan*, vol. 37, no. 5, pp. 645–649, 2004.
- [37] N. K. Swami, S. Srivastava, and H. M. Ghule, “The role of the interfacial layer in Schottky barrier solar cells,” *Journal of Physics D: Applied Physics*, vol. 12, no. 5, article 18, pp. 765–771, 1979.
- [38] C. M. H. Klimpke and P. T. Landsberg, “An improved analysis of the Schottky barrier solar cell,” *Solid State Electronics*, vol. 24, no. 5, pp. 401–406, 1981.
- [39] A. V. Rupa, D. Manikandan, D. Divakar, and T. Sivakumar, “Effect of deposition of Ag on TiO₂ nanoparticles on the photodegradation of Reactive Yellow-17,” *Journal of Hazardous Materials*, vol. 147, no. 3, pp. 906–913, 2007.



Hindawi

Submit your manuscripts at
<http://www.hindawi.com>

